Seawater pretreatment with an NF-like forward osmotic membrane: Membrane preparation, characterization and performance comparison with RO-like membranes

Zhikan Yao[a], Lu Elfa Peng[b], Hao Guo[b], Weihua Qing[b], Ying Mei[b] and Chuyang Y. Tang[b,*]

a. Key Laboratory of Biomass Chemical Engineering, College of Chemical and Biological Engineering, Zhejiang University, Hangzhou 310027, China.

b. Department of Civil Engineering, The University of Hong Kong, Pokfulam, Hong Kong S.A.R., China

*Corresponding author.

E-mail address: tangc@hku.hk (C.Y. Tang)

Abstract

A nanofiltration-like (NF-like) forward osmosis (FO) membrane was prepared by interfacial polymerization and applied for seawater pretreatment. The prepared NF-like FO membrane shows much higher water permeability and higher divalent salt to monovalent salt selectivity compared to a commercial reverse-osmotic-like (RO-like) FO membrane. The comparison between NF-like FO membrane and RO-like FO membrane in FO process was systematically investigated by using an antiscalent (sodium polyacrylate, PAANa) solution as draw solution. Both NF-like and RO-like FO process showed high rejection of alginate and sulfate. However, the water flux and monovalent salt (NaCl) passage in NF-like FO process were much higher, which enables the NF-like FO membrane to be a better candidate for pretreating seawater. The findings provide new insights on the design and preparation of FO membranes for seawater pretreatment.

Key words: Nanofiltration-like forward osmosis; reverse osmotic-like forward osmotic; desalination pretreatment; interfacial polymerization.

1. Introduction

Shortage in fresh water supply has led to the widespread practice of seawater desalination [1, 2]. Over the last few decades, reverse osmosis (RO) has become the leading desalination technology due to its simplicity of process configuration and relatively low energy consumption compared to thermal based desalination [3]. Priority research areas in RO based-desalination include process optimization [4, 5], high efficiency membrane preparation [6-9], and fouling mitigation [10-12].

Pretreatment is presumably the most critical strategy to mitigate fouling in seawater RO desalination [13, 14]. Compared to conventional pretreatment methods involving coagulation/medium filtration and their variations [15], membrane-based pretreatment such as microfiltration (MF) [16] and ultrafiltration (UF) [17] offers more compact footprint and better feed water quality. A recent survey shows that increasing number of modern seawater RO plants have adopted MF or UF in their pretreatment processes [18]. Several researchers have also explored the use of nanofiltration (NF) to pretreat seawater before RO desalination [14, 19, 20]. A common problem of these pressure-driven membrane processes used for pretreatment is that MF, UF, and NF themselves are prone to fouling, instability of flux, and thus demand for frequent cleaning and maintenance [21]. For example, it has been reported that fouling by natural organic matter could easily occur on NF membrane surfaces, which leads to greatly reduced water permeability [22-24].

Forward osmosis (FO) is an osmotic-pressure driven alternative to pressure-driven membrane processes. FO generally allows better flux stability and higher cleaning efficiency [25, 26]. Several research groups reported the use of FO for seawater pretreatment [27-31]. Existing literature in FO often emphasizes the critical importance of salt rejection (mainly NaCl rejection) - FO membranes mimicking the rejection properties of RO, i.e., RO-like FO membranes, are generally adopted [29]. Nevertheless, in an ideal FO-based pretreatment process, the membrane shall possess high water permeability to reduce its energy consumption. Although it is desirable to remove particulates, colloids, organic molecules, and divalent ions (e.g., Ca^{2+}, Mg^{2+} and SO_4^{2-}) to reduce the fouling and scaling potential of the pretreated seawater, we envisage an FO membrane with low NaCl rejection to minimize the trans-membrane osmotic pressure difference caused by the high concentration of NaCl in typical seawater. These design criteria for FO-based pretreatment prompt us to explore the use of NF-like FO membranes with high water permeability and nearly transparent to NaCl.

In this study, NF-like FO membranes with high divalent to monovalent salts selectivity were prepared for seawater pretreatment. We further explored the use of a polyelectrolyte sodium polyacrylate (PAANa), a commonly used antiscalant in seawater desalination, as the draw solution (DS). The pretreatment efficiency of this

NF-like FO process was systematically investigated using a synthetic seawater as the feed solution (FS), which shows greatly improved efficiency over conventional RO-like FO process. The findings in this study provide new insights on the design and preparation of FO membranes to enable high-efficiency seawater pretreatment.

2. Materials and methods

2.1 Materials

Polyacrylonitrile (PAN, M_w ~ 150,000), n,n-dimethylformamide (DMF, anhydrous 99.8%), piperazine (PIP, 99%), n-hexane (for HPLC, ≥ 95%), 1,3,5-benzenetricarbonyl trichloride (TMC, 98%) and sodium alginate (SA) were purchased from Sigma-Aldrich. Lithium chloride (LiCl, anhydrous) was obtained from TCI development Co., Ltd. Poly(acrylic acid) (PAA, 50% solution M_w ~ 3,000) was purchased from Aladdin®. Trisodium phosphate dodecahydrate (Na_3PO_4 •$12H_2O$), sodium chloride (NaCl, anhydrous), sodium sulfate (Na_2SO_4, anhydrous), sodium hydroxide (NaOH, anhydrous) and glucose (AR) were obtained from Dieckmann company. Deionized water (DI water) was supplied from a Milli-Q system (Millipore). PAA solution was neutralized to PAANa solution by adding theoretical amount of NaOH before using. RO-like FO (RO-FO) membranes used in this study were the thin film composite (TFC) FO membranes provided by Hydration Technology Innovations (HTI).

2.2 Membrane preparation

The PAN substrates were prepared through the non-solvent induced phase separation method [32]. The details for substrate preparation and characterization were shown in Supplementary Information S1. The NF-like FO (NF-FO) membranes were prepared by forming a rejection layer on PAN substrates via interfacial polymerization, a most widely applied method to prepare TFC membranes, following previously reported procedures [33]. Compared to cellulose acetate membranes, TFC membranes tend to have better separation performance [34]. Briefly, the PAN substrate was firstly immersed in a 1 wt% PIP with 0.6 wt% Na_3PO_4 (acid acceptor) aqueous solution for 2 min. After removing the excess PIP solution, the soaked substrate was dipped into 0.05 wt% TMC in n-hexane solution for 1 min. The resultant membrane was post-treated in DI water at 50 °C for 10 min. Finally, the prepared membrane was stored in DI water before characterization.

2.3 Membrane characterization

Morphologies of the prepared substrates and membranes were imaged by a Hitachi S-4800 field-emission scanning electron microscope (FE-SEM). Attenuated total reflectance Fourier transform infrared (ATR/FTIR) spectra were collected by a Thermo Fisher Scientific Nicolet 6700 ATR/FTIR spectroscope. To predict the surface hydrophilicity, the water contact angle of the substrates and membranes were obtained by an optical instrument (Attension Theta, Biolin Scientific). To evaluate the surface

charge properties, the surface zeta potentials and isoelectric point (IEP) of the substrates and membranes were measured by a SurPASS electrokinetic analyzer (SurPASS^{TM} 3, Anton Paar) following a standard operation [35].

Membrane intrinsic properties were evaluated in pressurized RO mode using a laboratory-scale cross-flow membrane filtration setup under 3 bar at around 25 °C [36]. DI water, and several types of aqueous solutions, such as NaCl solution (10 mmol/L), Na_2SO_4 solution (10 mmol/L), PAANa solution (10 mmol/L), SA solution (20 mg/L) or glucose (200 mg/L) were used as the feed solution. The pure water flux (J_v), pure water permeability (A), solute rejection (R) and separation factor (α) of Na_2SO_4 to NaCl were determined according to Eq. (1), Eq. (2), Eq. (3) and Eq. (4), respectively:

$$J_v = \frac{\Delta V}{\Delta t \times a} \qquad (1)$$

$$A = \frac{J_v}{\Delta p - \Delta \pi} \qquad (2)$$

$$R = \frac{C_f - C_p}{C_f} \times 100\% \qquad (3)$$

$$\alpha(NaCl/Na_2SO_4) = \frac{(C_{NaCl}/C_{Na2SO4})_p}{(C_{NaCl}/C_{Na2SO4})_f} = \frac{1-R_{NaCl}}{1-R_{Na2SO4}} \qquad (4)$$

where ΔV is the permeate water volume collected over a duration of Δt, a is the effective membrane area (42 cm^2 in this study), Δp is the hydraulic pressure difference across the membrane, $\Delta \pi$ is the osmotic pressure of the feed water, C_f and C_p, are the concentrations of the feed and permeate, respectively. In this study, concentration of inorganic salt was determined by conductivity meter (Ultrameter II, Myron L

company), and the concentration of SA and glucose was determined by a total organic carbon analyzer (TOC-V CPH, Shimadzu). The effective pore radius of the TFC membranes were estimated by applying solute transport method based on the apparent rejection of glucose [33, 37].

2.4 FO performance

The FO performances of the NF-FO membranes and RO-FO membranes were determined using a laboratory-scale cross-flow FO filtration system at around 25 °C [38]. All FO experiments were conducted in the active layer facing feed solution mode (ALFS mode or FO mode). Water flux (J_v) of the membrane was determined by measuring the weight changes of feed solution (FS) at regular time intervals according to Eq. (1). The solute rejection in FO (R_{FO}) was defined as Eq. (5) [39]:

$$R_{FO} = 1 - \frac{J_s}{J_v C_{fs}} \times 100\% \qquad (5)$$

where J_s and J_v are the solute and water flux in FO respectively, C_{fs} is the solute concentration in FS. J_s was obtained as the slope of plotted $C_{fs,t}$ $(V_{fs,0}$-J_v a $t)$ versus t [39], where $C_{fs,t}$ is the solute concentration in FS at t, $V_{fs,0}$ is the initial volume of FS, and a is the effective membrane area (42 cm^2 in this study). The solute concentration in feed solution (FS) was determined by conductivity meter and total organic carbon analyzer for the salts and the organics respectively.

To characterize the basic FO performance (water flux (J_v) and reverse solute flux (J_{rs})),

DI water was used as FS and PAANa solution over a concentration range of 1.17 mmol/L - 47.00 mmol/L were used as draw solution (DS). In this concentration range, PAANa solution has an osmotic pressure of 1.24 bar - 49.60 bar as estimated from the van't Hoff equation [40], which corresponds to the osmotic pressure generated by 0.025 M - 1 M NaCl solution. To evaluate the solute rejection in FO, NaCl solution (10 mmol/L), Na_2SO_4 solution (10 mmol/L), or SA solution (20 mg/L) were used as FS. To evaluate the FO performance for seawater pretreatment, a synthetic seawater containing NaCl (32 g/L), Na_2SO_4 (4 g/L) and SA (20 mg/L) was used. The DS contained PAANa (8.81 mmol/L) and NaCl (32 g/L).

3. Results and discussion

3.1 Membrane characterization

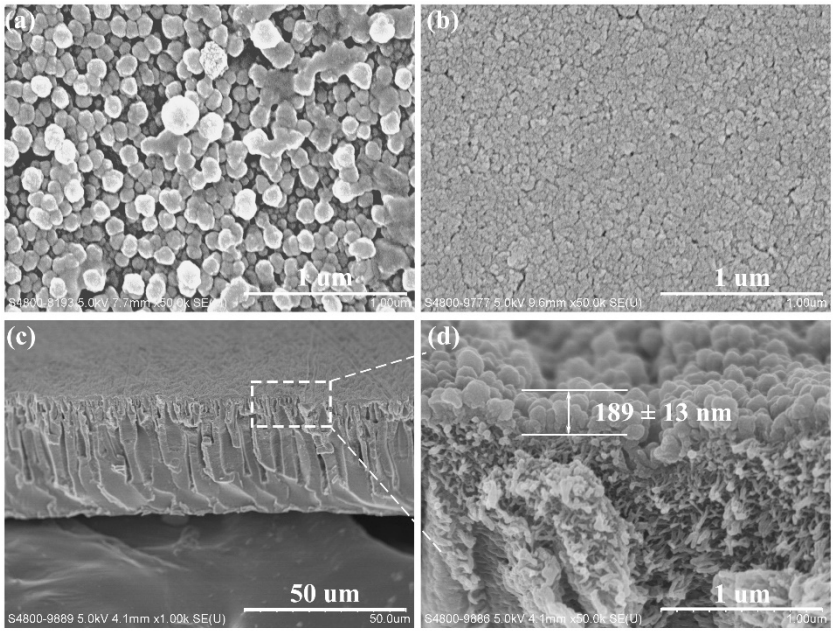

Figure 1 SEM images of the NF-FO membranes: top surface (a), bottom surface (b), cross-section with low magnification (c) and cross-section with high magnification

(d).

The top surface morphology of the NF-FO membrane (Fig. 1a) shows nodular surface morphologies that are typical for the PIP/TMC interfacial polymerization [33, 41]. Compared with PAN substrate (Fig. S1a), the NF-FO membrane contains an additional thin polyamide layer with a thickness on the order of 100 - 200 nm (Fig. 1d and Fig. S1d). Moreover, the porous bottom surface and finger-like cross-section structures of the NF-FO membrane are beneficial for reducing the structural parameter (191 μm for NF-FO, Table S1) and decreasing the influence of internal concentration polarization (ICP) in FO process [42-44].

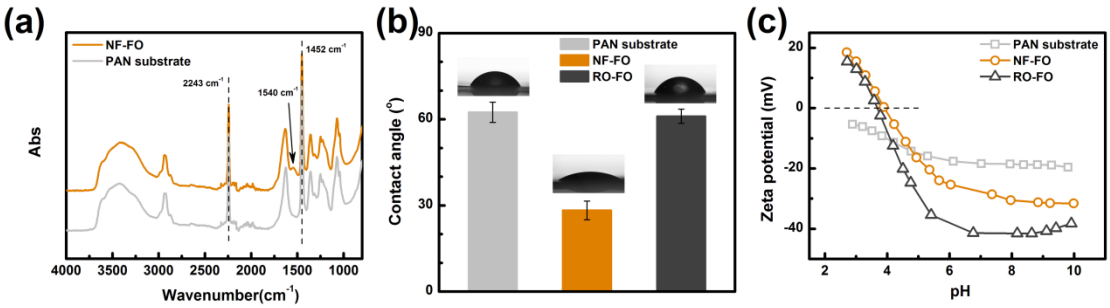

Figure 2 Membrane characterization results: the ATR/FTIR spectra (a) water contact angle results (b) and zeta potential curves (c) of the PAN substrate, NF-FO membrane and RO-FO membrane.

Fig. 2a shows the ATR/FTIR spectra of the PAN substrate and NF-FO membrane. The peaks at 2243 cm^{-1} and 1452 cm^{-1} were attributed to -CN stretching vibration and

-CH_2 bending vibration in the PAN polymer [45, 46]. Compared with the PAN substrate, a new peak at 1540 cm^{-1} appears in the spectrum of NF-FO membrane. It is ascribed to the amide II (C-N) stretching vibration which is a characteristic signal for polyamide groups formed by the interfacial polymerization of PIP and TMC [47]. This result consistent with the SEM results revealed the formation of polyamide rejection layer on PAN substrate.

The PAN substrate showed a hydrophilic surface with water contact angle of about 62.5 ± 3.5 ˚ (Fig. 2b). Preparing FO membrane on this hydrophilic substrate is desirable to allow water to penetrate the fine pores which could effectively reduce ICP and enhance water flux during FO process [43, 48]. The NF-FO membrane showed much lower water contact angle (28.3 ± 3.3 ˚) compared with the PAN substrate. These should be attributed to the formation of a hydrophilic polyamide layer by interfacial polymerization as well as the increasing of roughness which could be found in top surface SEM images (Fig. 1a and Fig. S1a). Moreover, the prepared NF-FO membrane showed much more hydrophilic than the commercial RO-FO membrane, which is in good agreement with the existing literature [38, 49]. This hydrophilic surface of NF-FO membrane could benefit the water transport through the membranes [33]. Both the NF-FO membrane and commercial RO-FO membrane are negatively charged at pH > 4 (Fig. 2c), which is due to the deprotonation of carboxylic groups, i.e., -COOH → $-COO^-$ + H^+. This negative membrane surface

charge is beneficial for the divalent ions (i.e. SO_4^{2-}) rejection by the membranes according to Donnan exclusion effect [50, 51].

3.2 Membrane separation properties

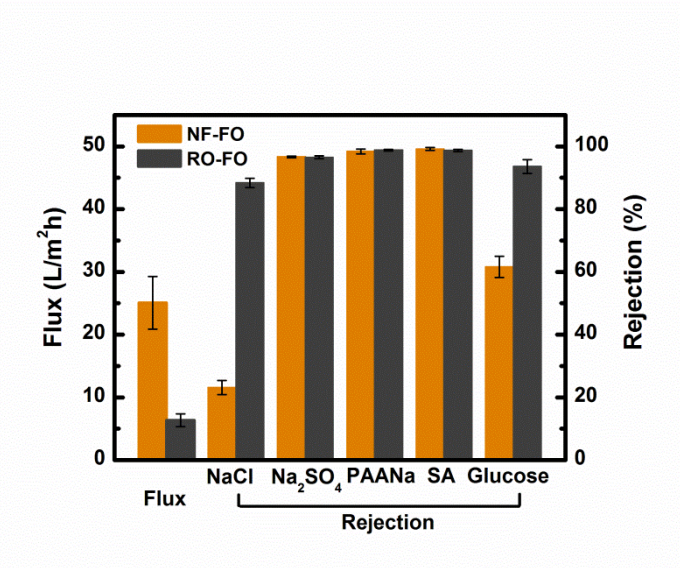

Figure 3 The water flux, solutes (NaCl, Na_2SO_4, PAANa, SA and glucose) rejection of NF-FO membrane and RO-FO membrane

Compared with RO-FO membrane, the NF-FO membrane showed higher water flux (Fig. 3). Correspondingly, the water permeability of the NF-FO membrane was approximately 4 times of that of the RO-FO membrane ($2.32 \pm 0.39 \times 10^{-11}$ m/s Pa vs. $0.59 \pm 0.09 \times 10^{-11}$ m/s Pa, Table S1). The NF-FO membrane had a significantly lower NaCl rejection but similar Na_2SO_4 rejection compared to its RO-like counterpart (Fig. 3), which led to a much higher divalent salt (Na_2SO_4) to monovalent salt (NaCl) selectivity (23.09 ± 1.35 for NF-FO vs. 3.36 ± 0.29 for RO-FO, Table S1). Meanwhile, both membranes showed high rejection to PAANa and SA (Fig. 3). Moreover, the

NF-FO membrane showed a lower rejection to the neutral molecule (glucose) compared with RO-FO membrane. Based on these neutral molecule rejection results, the pore radius of RO-FO membrane and NF-FO membrane were calculated as 0.47 ± 0.02 nm and 0.75 ± 0.03 nm, respectively (Table S1) [33, 37]. These results imply that: (1) both membranes are adequate for the removal of divalent ions and organic molecules, which is required in seawater pretreatment to abate the fouling and scaling risks [13], and (2) PAANa, a commonly used antiscalant in seawater desalination, can be potentially used as a draw solute thanks to its low reverse diffusion [52]. On the other hand, the significantly higher water permeability and higher divalent to monovalent salt selection could potentially allow improved water flux in typical FO operation (see Section 3.3 and 3.4).

3.3 FO performance

3.3.1 Water flux

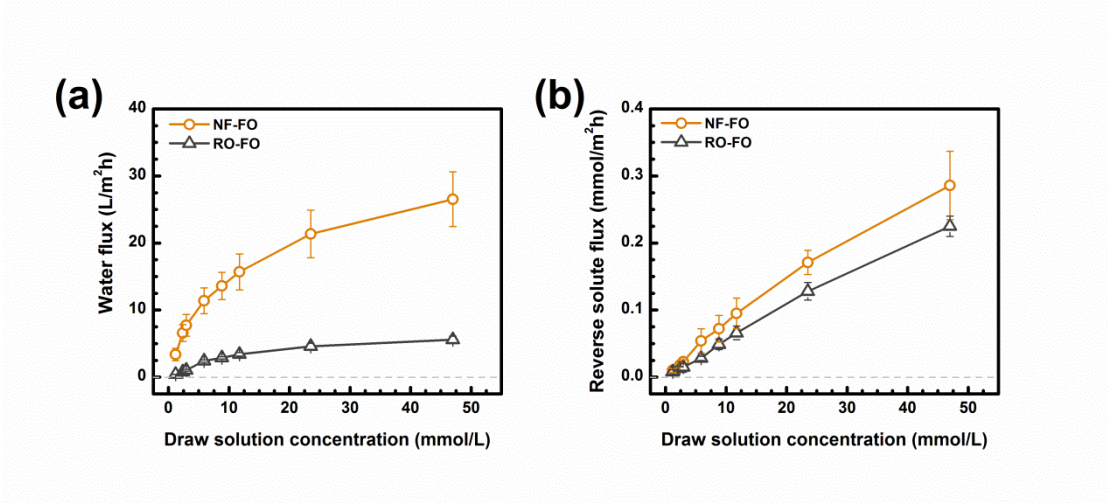

Figure 4 Effects of different DS concentration on (a) water flux and (b) reverse solute

flux of NF-FO membrane and RO-FO membrane.

Increasing DS concentration resulted in higher FO water flux for both membranes (Fig. 4a). Nevertheless, at any given DS (PAANa) concentration, the water flux of the NF-FO membrane was much higher than that of the RO-FO membrane (Fig. 4a), which is attributed to the much higher permeability of the former [49]. In addition, the FO water flux curve for the RO-FO membrane was much flatter, particularly over the high DS concentration range, which reveals the greater ICP experienced by this membrane. The reverse solute flux of the NF-FO membrane was slightly higher than that of the RO-FO membrane. Nevertheless, for both membranes, the maximum reverse solute flux was < 0.3 mmol/m^2h (Fig. 4b). According to a prior study [53], a slight amount of reverse permeated antiscalent might be helpful for reduce the scaling risk of the FO membranes.

3.3.2 Organic molecules rejection

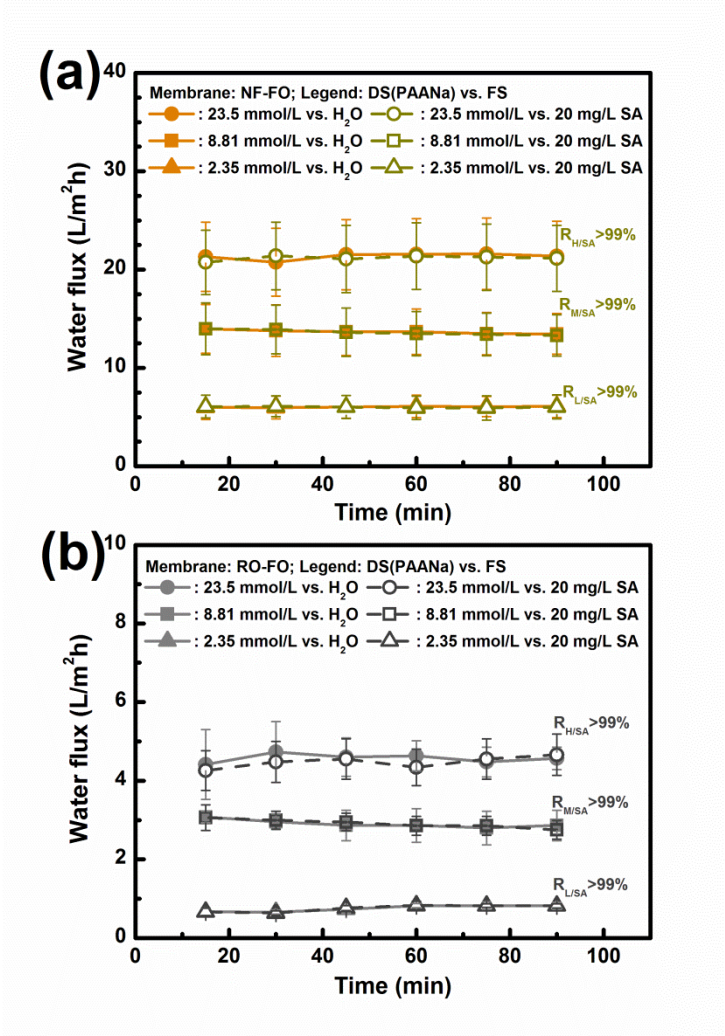

Figure 5 SA rejections and water flux variations in NF-FO process (a) and RO-FO process (b) driven by DS with low concentration (2.35 mmol/L), medium concentration (8.81 mmol/L) and high concentration (23.5 mmol/L). The FS used in the tests were DI water or SA solution (20 mg/L).

Regardless of the FO water flux level (achieved under various DS concentrations), the macromolecule SA can be adequately rejected by both membranes as > 99% (Fig. 5), which is beneficial for protecting the subsequent RO desalination process from

organic fouling [13]. Moreover, no significant water flux decreasing in the two FO processes were observed during the organic molecules rejection tests, which revealed the low fouling tendency of these two membranes in FO process.

3.3.3 Salts rejection in FO

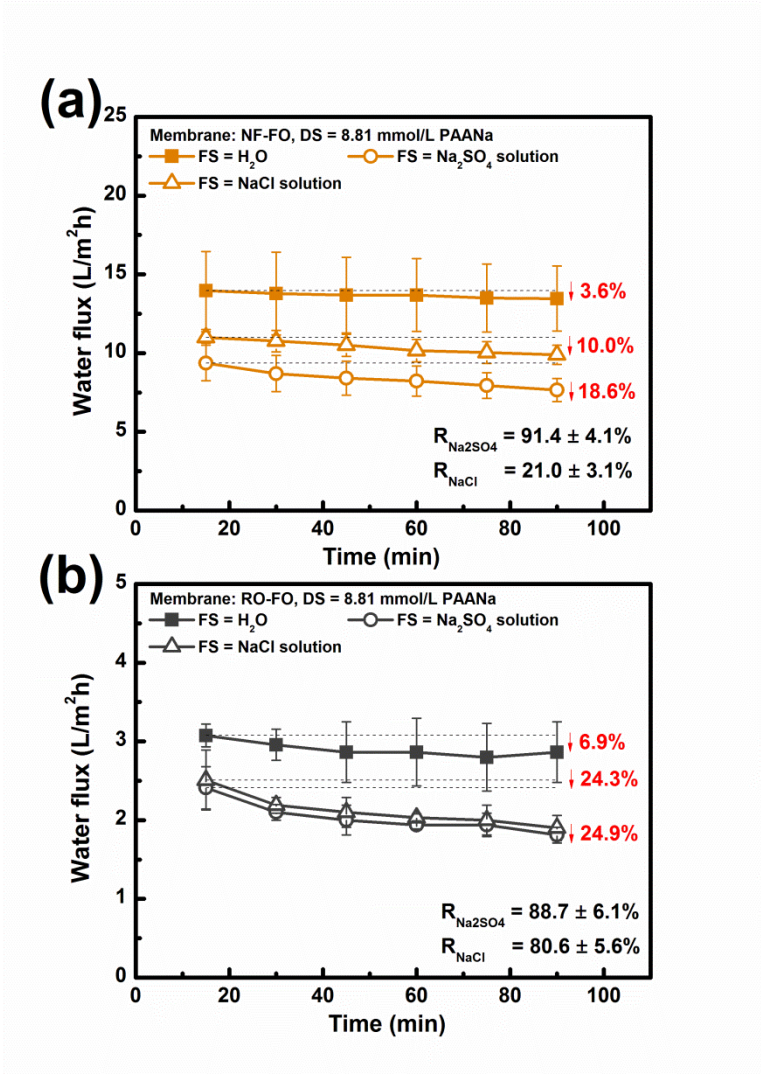

Figure 6 The water flux variations and salts rejections in NF-FO process (a) and RO-FO process (b) during the tests. Test conditions: PAANa solution with medium concentration (8.81 mmol/L) was used DS. DI water, Na_2SO_4 solution (10 mmol/L) or

NaCl solution (10 mmol/L) was used as FS.

Fig. 6 presents the FO water flux and salts rejection for FS containing 10 mmol/L NaCl or Na_2SO_4. The NF-FO membrane showed a high rejection of 91.4% for Na_2SO_4 and a low rejection of 21.0% for NaCl (Fig.6a). In contrast, the rejections to both Na_2SO_4 and NaCl by the RO-FO membrane were higher than 80% (Fig.6b). This general trend is in good agreement with the rejection results obtained under the pressurized RO testing mode (Fig. 3 and Table S1). The slightly high rejection of Na_2SO_4 under FO mode by the NF-FO membrane compared to the RO-FO membrane can be explained by its much higher water flux, i.e., the dilution effect [25, 33, 54]. In the current study, the RO-FO membrane had nearly identical FO water flux for FS containing 10 mM NaCl or 10 mM Na_2SO_4, due to their similar salt rejections by this membrane (80.6% for NaCl and 88.7% for Na2SO4, Fig.6b). In comparison, the FO water flux for NF-FO in the presence of 10 mM NaCl was significantly higher than that in the presence of 10 mM Na_2SO_4 (Fig. 6a). This contrast in flux behavior is resulted from the low NaCl rejection of the NF-FO membrane. With the lower rejection to NaCl, the effective osmotic pressure difference caused by NaCl across the NF-FO membrane greatly reduced, which thereby enhanced the FO water flux. This benefit is even more pronounced for FS containing higher NaCl concentration, a condition pertinent to seawater pretreatment (see Section 3.4).

3.4. Application in seawater pretreatment

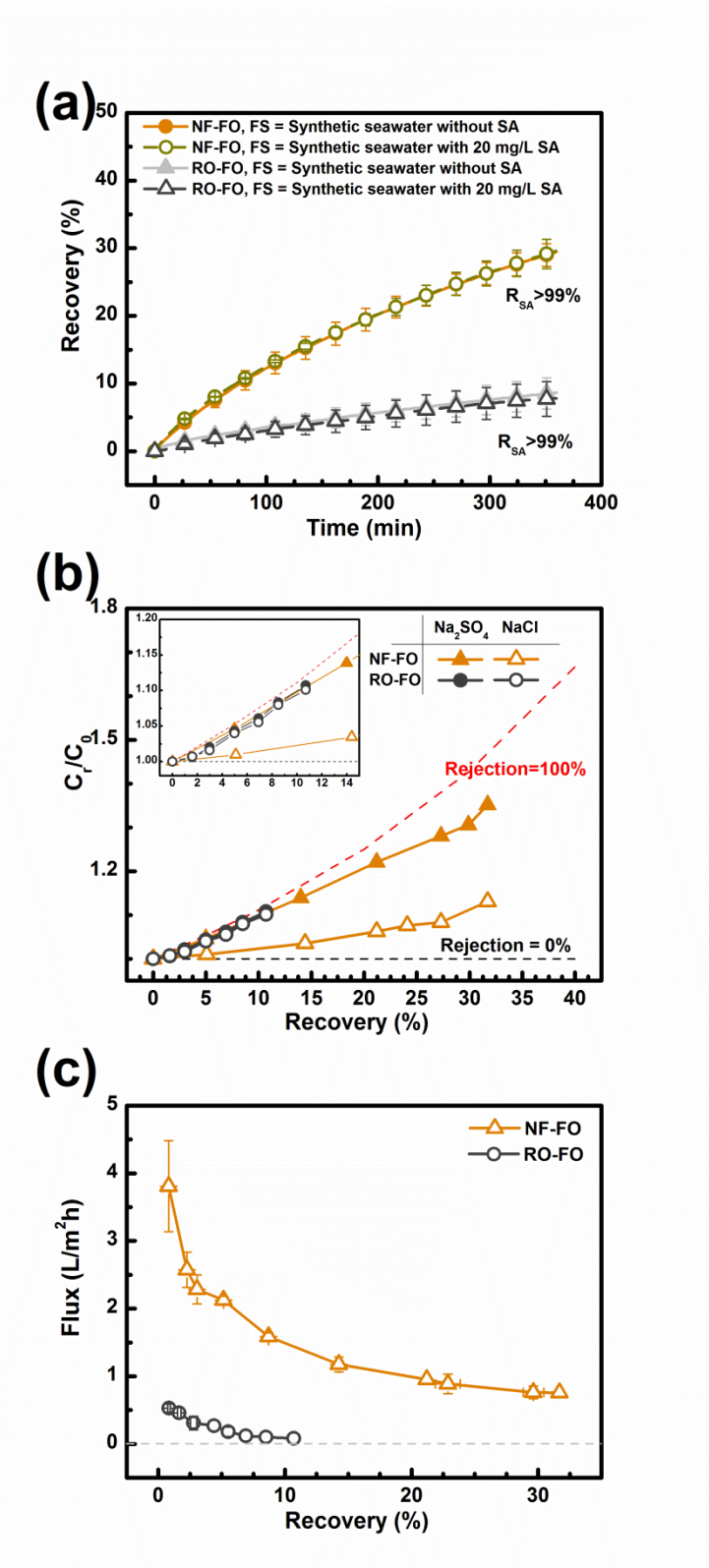

Figure 7 The comparison of NF-FO membrane and RO-FO membrane applied in the seawater pretreatment: (a) The feed recovery variation, (b) Na_2SO_4 and NaCl

concentration variations in FS, and (c) the water flux variations. Test conditions: NaCl (32g/L), Na_2SO_4 (4g/L) and SA (20 mg/L) mixed solution was used as FS. PAANa (8.81 mmol/L) and NaCl (32g/L) mixed solution was used DS.

Fig. 7 shows a comparison of NF-FO process and RO-FO process in synthetic seawater pretreatment. Within the 6 h batch tests, the NF-FO process was able to achieve significantly higher recovery compared to that of the RO-FO process (Fig. 7a). The presence of an organic macromolecule, SA, does not seem to affect the FO performance for both membranes, showing that organic fouling was not significant under the current study. Furthermore, both membranes had SA rejections of > 99% (Fig. 7a).

The solutes in the FS become more concentrated at increased recovery. Fig. 7b plots the concentration ratio (C_r/C_0) as a function of recovery, where C_r and C_0 are the feed solute concentration at a given recovery and the initial concentration, respectively. For comparison purpose, the theoretical curves corresponding to perfect solute rejection and zero solute rejection are also presented in the same figure. For the RO-FO membrane, both NaCl and Na_2SO_4 were concentrated nearly in accordance to the perfect-rejection curve, as a result of its high rejection to both solutes. However, the NaCl concentration in NF-FO process rose slowly which implied the advantages of NF-RO process in seawater pretreatment. When the recovery ratio was more than

30%, the NaCl concentration was only approximately 1.1 times of the initial value, which meant most of NaCl had passed through the NF-FO membrane.

With the increasing of the recovery ratio, the water flux of both the two FO process decreased (Fig. 7c). These could also be explained by osmotic pressure variation in FS and DS. More importantly, the water flux in NF-FO process was much higher compared with the one in RO-FO process, which is consistent with its higher water permeability and lower NaCl rejection.

4. Conclusion

NF-FO membrane was prepared by interfacial polymerization between PIP and TMC. The intrinsic separation properties of NF-FO membrane were tested in RO mode and compared with commercial RO-FO membrane. The NF-FO membrane showed high water permeability, organic molecules rejection and divalent salt to monovalent salt selectivity. The performance of NF-FO membrane in FO process was systematically investigated by using PAANa aqueous solution as draw solution and compered with RO-FO membrane. In FO process, NF-FO membrane also exhibited high water flux but low reverse PAANa flux, high organic molecules rejection and divalent salt rejection but low monovalent salt rejection, and low fouling potential. The advantage of NF-FO over RO-FO as a seawater pretreatment step is further confirmed based on batch tests using synthetic seawater. Future studies need to explore NF-like FO membranes with higher water permeability and nearly-zero NaCl rejection to further

unleash their potential for desalination pretreatment.

Appendix A. Supplementary information

This supplementary information includes the preparation and characterization of PAN substrates, intrinsic separation properties of NF-FO membrane and RO-FO membrane, **FO performance of NF-FO membrane and RO-FO membrane**.

Acknowledgements

The work described in this paper was partially supported by a grant from the Research Grants Council of the Hong Kong Special Administration Region, China (C7051-17G), and partially supported by the Fundamental Research Funds for the Central Universities, China (2019QNA4048). We also acknowledge the help on TOC analysis by Miss Vicky Fung and the RO-like FO membrane samples providing by HTI.

Reference

[1] M. Elimelech, W.A. Phillip, The future of seawater desalination: energy, technology, and the environment, Science, 333 (2011) 712-717.

[2] A. Subramani, J.G. Jacangelo, Emerging desalination technologies for water treatment: a critical review, Water Research, 75 (2015) 164-187.

[3] G. Amy, N. Ghaffour, Z. Li, L. Francis, R.V. Linares, T. Missimer, S. Lattemann,

Membrane-based seawater desalination: Present and future prospects, Desalination, 401 (2017) 16-21.

[4] L.F. Greenlee, D.F. Lawler, B.D. Freeman, B. Marrot, P. Moulin, Reverse osmosis desalination: water sources, technology, and today's challenges, Water Research, 43 (2009) 2317-2348.

[5] J. Kim, S. Hong, Optimizing seawater reverse osmosis with internally staged design to improve product water quality and energy efficiency, Journal of Membrane Science, 568 (2018) 76-86.

[6] X.-H. Ma, Z.-K. Yao, Z. Yang, H. Guo, Z.-L. Xu, C.Y. Tang, M. Elimelech, Nanofoaming of polyamide desalination membranes to tune permeability and selectivity, Environmental Science & Technology Letters, 5 (2018) 123-130.

[7] X.-H. Ma, Z. Yang, Z.-K. Yao, H. Guo, Z.-L. Xu, C.Y. Tang, Interfacial polymerization with electrosprayed microdroplets: Toward controllable and ultrathin polyamide membranes, Environmental Science & Technology Letters, 5 (2018) 117-122.

[8] M.R. Chowdhury, J. Steffes, B.D. Huey, J.R. McCutcheon, 3D printed polyamide membranes for desalination, Scinece, 361 (2018) 682-686.

[9] M. Shi, Z. Wang, S. Zhao, J. Wang, P. Zhang, X. Cao, A novel pathway for high performance RO membrane: Preparing active layer with decreased thickness and enhanced compactness by incorporating tannic acid into the support, Journal of Membrane Science, 555 (2018) 157-168.

[10] M.S. Rahaman, H. Thérien-Aubin, M. Ben-Sasson, C.K. Ober, M. Nielsen, M. Elimelech, Control of biofouling on reverse osmosis polyamide membranes modified with biocidal nanoparticles and antifouling polymer brushes, Journal of Materials Chemistry B, 2 (2014) 1724.

[11] S. Jiang, Y. Li, B.P. Ladewig, A review of reverse osmosis membrane fouling and control strategies, The Science of the Total Environment, 595 (2017) 567-583.

[12] Y. Baek, B.D. Freeman, A.L. Zydney, J. Yoon, A facile surface modification for antifouling reverse osmosis membranes using polydopamine under UV irradiation, Industrial & Engineering Chemistry Research, 56 (2017) 5756-5760.

[13] S. Jamaly, N.N. Darwish, I. Ahmed, S.W. Hasan, A short review on reverse osmosis pretreatment technologies, Desalination, 354 (2014) 30-38.

[14] D. Zhou, L. Zhu, Y. Fu, M. Zhu, L. Xue, Development of lower cost seawater desalination processes using nanofiltration technologies — A review, Desalination, 376 (2015) 109-116.

[15] S.A. Alizadeh Tabatabai, J.C. Schippers, M.D. Kennedy, Effect of coagulation on fouling potential and removal of algal organic matter in ultrafiltration pretreatment to seawater reverse osmosis, Water Research, 59 (2014) 283-294.

[16] B.S. Oh, H.Y. Jang, J. Cho, S. Lee, E. Lee, I.S. Kim, T.M. Hwang, Joon-WunKang, Effect of ozone on microfiltration as a pretreatment of seawater reverse osmosis, Desalination, 238 (2009) 90-97.

[17] J. Xu, G. Ruan, X. Gao, X. Pan, B. Su, C. Gao, Pilot study of inside-out and

outside-in hollow fiber UF modules as direct pretreatment of seawater at low temperature for reverse osmosis, Desalination, 219 (2008) 179-189.

[18] C.Y. Tang, Z. Yang, H. Guo, J.J. Wen, L.D. Nghiem, E. Cornelissen, Potable water reuse through advanced membrane technology, Environmental Science & Technology, 52 (2018) 10215-10223.

[19] B. Su, T. Wu, Z. Li, X. Cong, X. Gao, C. Gao, Pilot study of seawater nanofiltration softening technology based on integrated membrane system, Desalination, 368 (2015) 193-201.

[20] Y. Song, B. Su, X. Gao, C. Gao, The performance of polyamide nanofiltration membrane for long-term operation in an integrated membrane seawater pretreatment system, Desalination, 296 (2012) 30-36.

[21] R. Zhang, Y. Liu, M. He, Y. Su, X. Zhao, M. Elimelech, Z. Jiang, Antifouling membranes for sustainable water purification: strategies and mechanisms, Chemical Society Reviews, 45 (2016) 5888-5924.

[22] S. Hong, M. Elimelech, Chemical and physical aspects of natural organic matter (NOM) fouling of nanofiltration membranes, Journal of Membrane Science, 132 (1997) 159-181.

[23] A. Seidel, M. Elimelech, Coupling between chemical and physical interactions in natural organic matter (NOM) fouling of nanofiltration membranes: Implications for fouling control, Journal of Membrane Science, 203 (2002) 245-255.

[24] Q. Li, M. Elimelech, Organic fouling and chemical cleaning of nanofiltration

membranes: Measurements and mechanisms, Environmental Science & Technology, 38 (2004) 4683-4693.

[25] T. Cath, A. Childress, M. Elimelech, Forward osmosis: Principles, applications, and recent developments, Journal of Membrane Science, 281 (2006) 70-87.

[26] S. Zhao, L. Zou, C.Y. Tang, D. Mulcahy, Recent developments in forward osmosis: Opportunities and challenges, Journal of Membrane Science, 396 (2012) 1-21.

[27] N.T. Hancock, P. Xu, D.M. Heil, C. Bellona, T.Y. Cath, Comprehensive bench- and pilot-scale investigation of trace organic compounds rejection by forward osmosis, Environmental Science & Technology, 45 (2011) 8483-8490.

[28] D. Zhao, P. Wang, Q. Zhao, N. Chen, X. Lu, Thermoresponsive copolymer-based draw solution for seawater desalination in a combined process of forward osmosis and membrane distillation, Desalination, 348 (2014) 26-32.

[29] A. Altaee, G. Zaragoza, H.R. van Tonningen, Comparison between forward osmosis-reverse osmosis and reverse osmosis processes for seawater desalination, Desalination, 336 (2014) 50-57.

[30] L. Chekli, S. Phuntsho, J.E. Kim, J. Kim, J.Y. Choi, J.-S. Choi, S. Kim, J.H. Kim, S. Hong, J. Sohn, H.K. Shon, A comprehensive review of hybrid forward osmosis systems: Performance, applications and future prospects, Journal of Membrane Science, 497 (2016) 430-449.

[31] B.G. Choi, M. Zhan, K. Shin, S. Lee, S. Hong, Pilot-scale evaluation of FO-RO

osmotic dilution process for treating wastewater from coal-fired power plant integrated with seawater desalination, Journal of Membrane Science, 540 (2017) 78-87.

[32] Z. Yao, Y. Cui, K. Zheng, B. Zhu, L. Zhu, Composition and properties of porous blend membranes containing tertiary amine based amphiphilic copolymers with different sequence structures, Journal of Colloid and Interface Science, 437 (2015) 124-131.

[33] Z. Yao, H. Guo, Z. Yang, W. Qing, C.Y. Tang, Preparation of nanocavity-contained thin film composite nanofiltration membranes with enhanced permeability and divalent to monovalent ion selectivity, Desalination, 445 (2018) 115-122.

[34] X. Wang, Y. Zhao, B. Yuan, Z. Wang, X. Li, Y. Ren, Comparison of biofouling mechanisms between cellulose triacetate (CTA) and thin-film composite (TFC) polyamide forward osmosis membranes in osmotic membrane bioreactors, Bioresource Technology, 202 (2016) 50-58.

[35] Z. Yao, S. Du, Y. Zhang, B. Zhu, L. Zhu, A.E. John, Positively charged membrane for removing low concentration Cr(VI) in ultrafiltration process, Journal of Water Process Engineering, 8 (2015) 99-107.

[36] Z. Yao, H. Guo, Z. Yang, C. Lin, B. Zhu, Y. Dong, C.Y. Tang, Reactable substrate participating interfacial polymerization for thin film composite membranes with enhanced salt rejection performance, Desalination, 436 (2018) 1-7.

[37] W.R. Bowen, A.W. Mohammad, N. Hilal, Characterisation of nanofiltration membranes for predictive purposes - Use of salts, uncharged solutes and atomic force microscopy, Journal of Membrane Science, 126 (1997) 91-105.

[38] H. Guo, Z. Yao, J. Wang, Z. Yang, X. Ma, C.Y. Tang, Polydopamine coating on a thin film composite forward osmosis membrane for enhanced mass transport and antifouling performance, Journal of Membrane Science, 551 (2018) 234-242.

[39] X. Jin, Q. She, X. Ang, C.Y. Tang, Removal of boron and arsenic by forward osmosis membrane: Influence of membrane orientation and organic fouling, Journal of Membrane Science, 389 (2012) 182-187.

[40] D.J. Johnson, W.A. Suwaileh, A.W. Mohammed, N. Hilal, Osmotic's potential: An overview of draw solutes for forward osmosis, Desalination, 434 (2018) 100-120.

[41] Y. Li, Y. Su, J. Li, X. Zhao, R. Zhang, X. Fan, J. Zhu, Y. Ma, Y. Liu, Z. Jiang, Preparation of thin film composite nanofiltration membrane with improved structural stability through the mediation of polydopamine, Journal of Membrane Science, 476 (2015) 10-19.

[42] J. Wei, C. Qiu, C.Y. Tang, R. Wang, A.G. Fane, Synthesis and characterization of flat-sheet thin film composite forward osmosis membranes, Journal of Membrane Science, 372 (2011) 292-302.

[43] Q. Saren, C.Q. Qiu, C.Y. Tang, Synthesis and characterization of novel forward osmosis membranes based on layer-by-layer assembly, Environmental Science & Technology, 45 (2011) 5201-5208.

[44] B. Kim, G. Gwak, S. Hong, Review on methodology for determining forward osmosis (FO) membrane characteristics: Water permeability (A), solute permeability (B), and structural parameter (S), Desalination, 422 (2017) 5-16.

[45] X. Weng, Y. Ji, F. Zhao, Q. An, C. Gao, Tailoring the structure of polyamide thin film composite membrane with zwitterions to achieve high water permeability and antifouling property, RSC Advances, 5 (2015) 98730-98739.

[46] C. Qiu, S. Qi, C.Y. Tang, Synthesis of high flux forward osmosis membranes by chemically crosslinked layer-by-layer polyelectrolytes, Journal of Membrane Science, 381 (2011) 74-80.

[47] A.P. Rao, S.V. Joshi, J.J. Trivedi, C.V. Devmurari, V.J. Shah, Structure–performance correlation of polyamide thin film composite membranes effect of coating conditions on film formation, Journal of Membrane Science, 211 (2003) 13-24.

[48] J.R. McCutcheon, M. Elimelech, Influence of membrane support layer hydrophobicity on water flux in osmotically driven membrane processes, Journal of Membrane Science, 318 (2008) 458-466.

[49] J. Wei, C. Qiu, Y.-N. Wang, R. Wang, C.Y. Tang, Comparison of NF-like and RO-like thin film composite osmotically-driven membranes—Implications for membrane selection and process optimization, Journal of Membrane Science, 427 (2013) 460-471.

[50] M. Paul, S.D. Jons, Chemistry and fabrication of polymeric nanofiltration

membranes: A review, Polymer, 103 (2016) 417-456.

[51] Z. Yao, Z. Yang, H. Guo, X. Ma, Y. Dong, C.Y. Tang, Highly permeable and highly selective ultrathin film composite polyamide membranes reinforced by reactable polymer chains, Journal of Colloid and Interface Science, 552 (2019) 418-425.

[52] Q. Ge, J. Su, G.L. Amy, T.S. Chung, Exploration of polyelectrolytes as draw solutes in forward osmosis processes, Water Research, 46 (2012) 1318-1326.

[53] G. Gwak, S. Hong, New approach for scaling control in forward osmosis (FO) by using an antiscalant-blended draw solution, Journal of Membrane Science, 530 (2017) 95-103.

[54] Z. Yang, H. Guo, C.Y. Tang, The upper bound of thin-film composite (TFC) polyamide membranes for desalination, Journal of Membrane Science, 590 (2019) 117297.

Supplementary Information

NF-like forward osmotic membrane for desalination pretreatment: Preparation, characterization and comparison with RO-like membrane

Zhikan Yao[a], Lu Elfa Peng[b], Hao Guo[b], Weihua Qing[b], Ying Mei[b] and Chuyang Y. Tang[b,*]

a. Key Laboratory of Biomass Chemical Engineering, College of Chemical and Biological Engineering, Zhejiang University, Hangzhou 310027, China.

b. Department of Civil Engineering, The University of Hong Kong, Pokfulam, Hong Kong S.A.R., China

*Corresponding author.

E-mail address: tangc@hku.hk (C.Y. Tang)

S1 Preparation and characterization of PAN substrate

The PAN substrates were prepared through the non-solvent induced phase separation (NIPS) method [1]. In a typical preparation process, PAN (16 wt%) and LiCl (2 wt%) were firstly dissolved in DMF (82 wt%) to prepare a casting solution. Then the casting solution was spread into a 150 μm thick thin liquid film on a glass plate by an automatic film applicator (Elcometer 4340, Elcometer). Afterwards, the nascent film was coagulated in a deionized water bath at about 25 °C. Finally, the formed substrate was stored in deionized water before use. The top surface, bottom surface and cross-section morphologies of the prepared PAN substrate were imaged by SEM and showed in Fig. S1. This substrate showed porous surface and finger-like cross-section structure. This PAN substrate also showed high porosity (80.7% ± 5.6%, tested by liquid displacement method [2]) and thin thickness (71.4 ± 4.1 μm, tested in wet state by a micrometer). A pure water filtration test was carried out on the substrate at 1 bar. The water flux of the substrate was about 198.3 ± 8.1 L/m^2h.

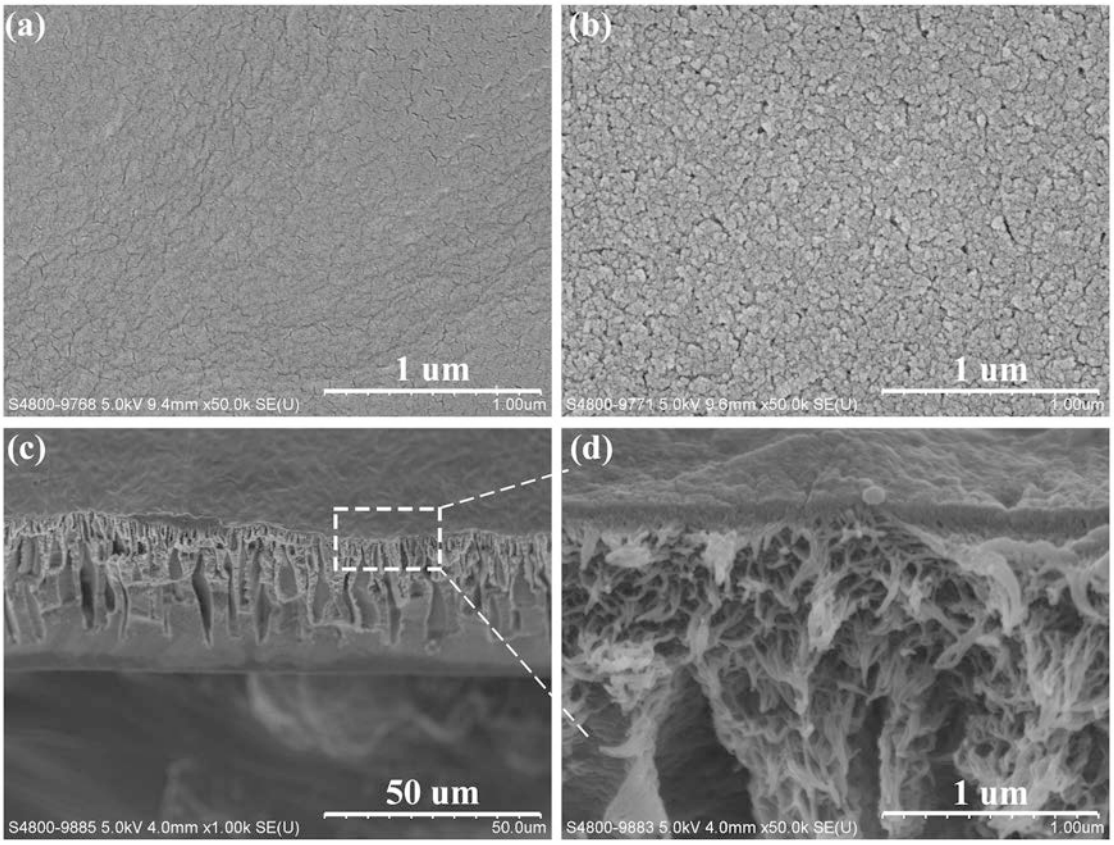

Figure S1 Top surface (a), bottom surface (b), cross-section with low magnification (c) and cross-section with high magnification (d) SEM images of the PAN substrate.

S2 Filtration properties of NF-FO membrane and RO-FO membrane

Table S1 Intrinsic separation properties and structure parameters of NF-FO membrane and RO-FO membrane.

Membrane	A ($\times10^{-11}$ m/s Pa)	α(NaCl/ Na_2SO_4)	B_{NaCl} ($\times10^{-7}$ m/s)	B_{Na2SO4} ($\times10^{-7}$ m/s)	B_{PAANa} ($\times10^{-7}$ m/s)	Effective pore radius (nm)	S value (μm)
NF-FO	2.32 ± 0.39	23.09 ± 1.35	196.90 ± 53.50	1.83 ± 0.44	0.73 ± 0.04	0.75 ± 0.03	191

RO-FO	0.59 ± 0.09	3.36 ± 0.29	1.97 ± 0.54	0.49 ± 0.14	0.19 ± 0.01	0.47 ± 0.02	426

The intrinsic separation properties of the NF-FO membrane and RO-FO membrane were calculated based on the results of membrane performance tests in RO mode and listed in Table S1. Compared with the RO-FO membrane, the NF-FO membrane showed high water permeability (A), NaCl permeability (B_{NaCl}) and divalent salt (Na_2SO_4) to monovalent salt (NaCl) selectivity. Meanwhile, both the two membranes showed low Na_2SO_4 and PAANa permeability (B_{Na2SO4} and B_{PAANa}). The effective pore radius [3, 4] and structure parameters (S value) [5] of the NF-FO membrane and RO-FO membrane were also calculated (Table S1). Compared with the RO-FO membrane, the NF-FO membrane showed much higher water permeability and much smaller S value, both contributed to greater FO water flux observed in the current study.

S3 FO performance of NF-FO membrane and RO-FO membrane

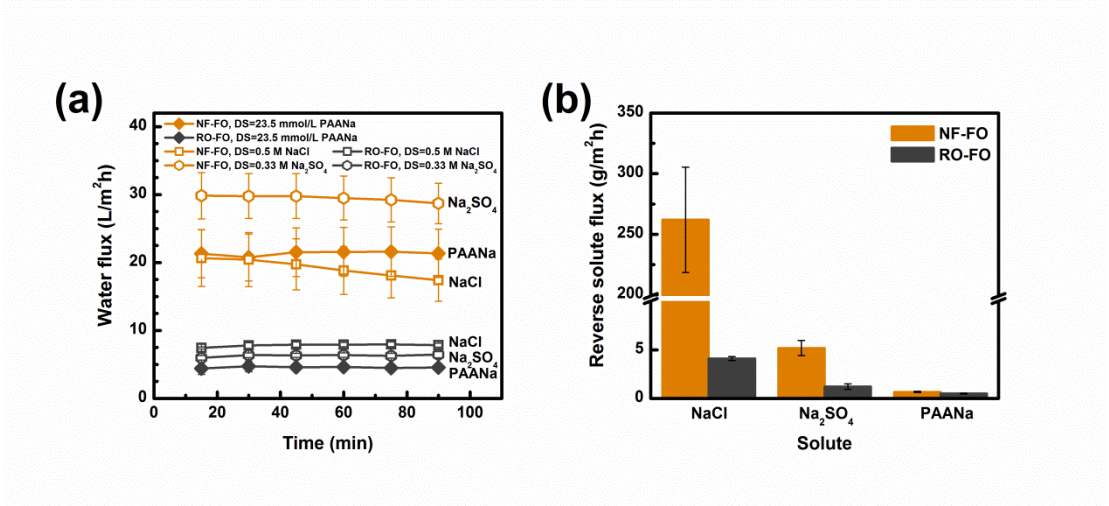

Figure S2 The water flux (a) and reverse solute flux (b) in NF-FO process and RO-FO process.

According to the van't Hoff equation [6], three different solutions (0.5M NaCl, 0.33M Na_2SO_4 or 23.5 mmol/L PAANa) with theoretically similar osmotic pressure were used as draw solutions to drive the FO process. Deionized water was used as feed solution. When the FO process was driven by the same draw solution, the NF-FO process performed much higher water flux, compared with the RO-FO process (Fig. S2a). During the testing period, the water flux in NF-FO process remained stable, when using Na_2SO_4 solution (0.33M) or PAANa solution (23.5 mmol/L) as draw solution. But the water flux in NF-FO process decreased gradually when using NaCl solution (0.5M) as draw solution. The water flux decreasing in the NF-FO process driven by NaCl solution (0.5M) could be explained by the high reverse salt flux shown in Fig. 2b. The water flux in RO-FO process remained stable, when NaCl solution (0.5M), Na_2SO_4 solution (0.33M) or PAANa solution (23.5 mmol/L) were used as draw solution.

It can also be found from Fig. 2b that, the reverse Na_2SO_4 and PAANa fluxes in NF-FO process and RO-FO process were all lower than about 6 g/m^2h. However, the reverse NaCl flux in NF-FO process was more than 60 times higher than the one in RO-FO process. It implied that Na_2SO_4 and PAANa could hardly pass through both the NF-FO membrane and RO-FO membrane; NaCl could be rejected by RO-FO

membrane but could easily pass through the NF-FO membrane.

References

[1] Z. Yao, Y. Cui, K. Zheng, B. Zhu, L. Zhu, Composition and properties of porous blend membranes containing tertiary amine based amphiphilic copolymers with different sequence structures, Journal of Colloid and Interface Science, 437 (2015) 124-131.

[2] Z. Yao, S. Du, Y. Zhang, B. Zhu, L. Zhu, A.E. John, Positively charged membrane for removing low concentration Cr(VI) in ultrafiltration process, Journal of Water Process Engineering, 8 (2015) 99-107.

[3] W.R. Bowen, A.W. Mohammad, N. Hilal, Characterisation of nanofiltration membranes for predictive purposes - Use of salts, uncharged solutes and atomic force microscopy, Journal of Membrane Science, 126 (1997) 91-105.

[4] Z. Yao, H. Guo, Z. Yang, W. Qing, C.Y. Tang, Preparation of nanocavity-contained thin film composite nanofiltration membranes with enhanced permeability and divalent to monovalent ion selectivity, Desalination, 445 (2018) 115-122.

[5] A. Tiraferri, N.Y. Yip, A.P. Straub, S. Romero-Vargas Castrillon, M. Elimelech, A method for the simultaneous determination of transport and structural parameters of forward osmosis membranes, Journal of Membrane Science, 444 (2013) 523-538.

[6] D.J. Johnson, W.A. Suwaileh, A.W. Mohammed, N. Hilal, Osmotic's potential: An overview of draw solutes for forward osmosis, Desalination, 434 (2018) 100-120.